Phosphorylated K-Ras limits cell survival by blocking Bcl-xL sensitization of inositol trisphosphate receptors

Pamela J. Sung[a], Frederick D. Tsai[a], Horia Vais[b], Helen Court[a], Jun Yang[b], Nicole Fehrenbacher[a], J. Kevin Foskett[b,c], and Mark R. Philips[a,1]

[a]New York University (NYU) Cancer Institute, NYU School of Medicine, New York, NY 10016; and Departments of [b]Physiology and [c]Cell and Developmental Biology, University of Pennsylvania, Philadelphia, PA 19014

Edited* by Joseph Schlessinger, Yale University School of Medicine, New Haven, CT, and approved November 6, 2013 (received for review April 15, 2013)

K-Ras4B is targeted to the plasma membrane by a farnesyl modification that operates in conjunction with a polybasic domain. We characterized a farnesyl-electrostatic switch whereby protein kinase C phosphorylates K-Ras4B on serine 181 in the polybasic region and thereby induces translocation from the plasma membrane to internal membranes that include the endoplasmic reticulum (ER) and outer mitochondrial membrane. This translocation is associated with cell death. Here we have explored the mechanism of phospho–K-Ras4B toxicity and found that GTP-bound, phosphorylated K-Ras4B associates with inositol trisphosphate receptors on the ER in a Bcl-xL–dependent fashion and, in so doing, blocks the ability of Bcl-xL to potentiate the $InsP_3$ regulated flux of calcium from ER to mitochondria that is required for efficient respiration, inhibition of autophagy, and cell survival. Thus, we have identified inositol trisphosphate receptors as unique effectors of K-Ras4B that antagonize the prosurvival signals of other K-Ras effectors.

oncogene | cancer | membrane protein

Ras proteins are mutated more frequently in human cancer than any other oncogene (1). Four Ras proteins are generated from three Ras genes because the transcript of the *kras* locus is alternatively spliced. Because Ras-dependent cancers most often harbor a mutation in *kras* (2), unique properties of the K-Ras proteins may prove useful in developing anti-Ras therapeutics.

Ras proteins differ substantially only in their C-terminal 23–24 amino acids, which constitute the hypervariable regions (HVRs) that target Ras proteins to membranes (3). The HVR includes the C-terminal CAAX motif, which is modified by farnesylation, proteolysis, and carboxyl methylation (3). However, these modifications are insufficient to stably target Ras proteins to membranes (4). Three of the four Ras isoforms also require palmitoylation at cysteines in the HVR. K-Ras4B is unique among Ras proteins in that it lacks modification with palmitate. Instead, this isoform augments the membrane affinity afforded by the farnesyl modification with a nearby polylysine motif that forms an electrostatic interaction with the negatively charged headgroups of the phospholipids of the inner leaflet of the plasma membrane (5).

We recently found that phosphorylation by protein kinase C (PKC) of serine 181 (S181) within the polybasic region of K-Ras4B neutralized the positive charge to a sufficient degree to promote release from the plasma membrane and cause accumulation of the GTPase on internal membranes (6). We coined the term "farnesyl-electrostatic switch" for this membrane release mechanism (7). When the farnesyl-electrostatic switch is engaged by stimulating PKC or substituting a phosphomimetic residue for serine 181, phospho–K-Ras4B translocates from the plasma membrane to the endoplasmic reticulum (ER), Golgi apparatus, and outer mitochondrial membrane (OMM) (6). Unexpectedly, this translocation is associated with markedly diminished survival of cells, suggesting a unique strategy for anti-Ras therapeutics.

Preliminary studies implicated apoptosis in phospho–K-Ras4B–mediated toxicity because a fluorescent biosensor for caspase-3 activation reported activity in cells expressing phospho–K-Ras (6). Paradoxically, Bcl-xL was required for phospho–K-Ras4B–stimulated cell death, suggesting a functional interaction between K-Ras4B and Bcl-xL that interferes with a survival pathway (6). Here we have sought to characterize the mechanism whereby phosphorylation of K-Ras4B on serine 181 impairs cell survival. We found that the organelle upon which K-Ras4B acts to limit survival is the ER where phospho–K-Ras4B interacts with inositol trisphosphate ($InsP_3$) receptors (IP3Rs). This interaction interferes with the ability of Bcl-xL to promote the IP3R-mediated transfer of calcium from the ER to mitochondria where this divalent cation is required for efficient respiration. We also found that phospho–K-Ras4B expression did not activate the intrinsic pathway of apoptosis but was associated with the induction of autophagy. Our data indicate that IP3R is a previously unappreciated effector of K-Ras4B that mediates the toxicity observed upon phospho–K-Ras expression.

Results

Phospho-K-Ras Limits Cell Survival from the ER. Whereas phosphorylation of K-Ras4B on serine 181 was associated with translocation to the OMM and diminished cell survival suggesting apoptosis (6), subsequent analysis failed to produce evidence of programmed cell death (Fig. S1). Most compelling of these results was the ability of K-Ras12V181E to limit cell survival in murine embryonic fibroblasts (MEFs) deficient in both Bax and Bak, which are deficient in apoptosis driven by mitochondrial dysfunction (8). We therefore sought a qualitative, apoptosis-independent assay for phospho–K-Ras–induced toxicity and developed a clonogenic assay that assesses the ability of cells stably expressing K-Ras or mutations thereof to survive in culture and grow to confluence (*Materials and Methods*). Using this assay, we found that, whereas wild-type (WT) MEFs are sensitive to phosphomimetic K-Ras12V181E, Bcl-xL-deficient MEFs (Bcl-$xL^{-/-}$) were protected. Importantly, toxicity could be restored by expression

Significance

K-Ras is mutated more often than any other oncogene, making the protein and the pathways it regulates attractive targets for anticancer drug discovery. We have shown that phosphorylation of serine 181 in the membrane-targeting region of K-Ras causes the protein to translocate from plasma membrane to intracellular membranes. Translocation is associated with toxicity but the mechanism has remained undefined. Here we show that phospho–K-Ras associates with inositol trisphosphate receptors (IP3Rs) on the endoplasmic reticulum (ER) and thereby blocks one of the prosurvival activities of Bcl-xL, which is to sensitize IP3Rs and thereby allow constitutive transfer of calcium from ER to mitochondria where it is required for efficient respiration. This pathway could be exploited to limit the oncogenic activity of mutant K-Ras.

Author contributions: P.J.S., J.K.F., and M.R.P. designed research; P.J.S., F.D.T., H.V., H.C., J.Y., and N.F. performed research; P.J.S., F.D.T., H.V., H.C., J.Y., N.F., J.K.F., and M.R.P. analyzed data; and P.J.S., J.K.F., and M.R.P. wrote the paper.

The authors declare no conflict of interest.

*This Direct Submission article had a prearranged editor.

[1]To whom correspondence should be addressed. E-mail: philim01@med.nyu.edu.

This article contains supporting information online at www.pnas.org/lookup/suppl/doi:10.1073/pnas.1306431110/-/DCSupplemental.

of exogenous Bcl-xL (Fig. S2*A*). To confirm that PKC-mediated phosphorylation of endogenous K-Ras has similar effects as ectopic expression of the phosphomimetic form, we used a pair of cell lines derived from HCT116 human colon cancer cells that are hemizygous for either WT K-Ras or oncogenic K-Ras13D, but isogenic at all other loci (9). Whereas HCT116 K-Ras WT cells were insensitive to PKC agonists, these agents inhibited the growth of HCT116 K-Ras13D cells (Fig. S2*B*), suggesting that phosphorylation of activated K-Ras limits growth.

Because phospho–K-Ras translocates to multiple internal membranes, including the Golgi apparatus, ER, and OMM (6), we sought to determine which, if any, of these subcellular locations are associated with toxicity. Using ectopic targeting sequences (viral M1 protein or yeast Mas70) we stringently targeted K-Ras to the ER (10) or OMM (11), the two compartments upon which Bcl-xL is known to function (12). To assure a GTP-bound conformation, the targeted constructs incorporated an activating G12V substitution. This mutation also enabled us to monitor the subcellular distribution of the proteins with a YFP-tagged Raf-1 Ras binding domain (RBD) probe (YFP-RBD) that binds with high affinity to activated Ras. YFP-RBD localization demonstrated that, whereas natively targeted K-Ras12V was predominantly at the plasma membrane, M1–K-Ras12V was restricted to the ER and Mas70–K-Ras12V was expressed on mitochondria (Fig. 1*A*). The results with YFP-RBD also demonstrated that the ectopically targeted K-Ras proteins folded properly and retained the ability to interact with effectors.

NIH 3T3 fibroblasts transduced under conditions of hygromycin selection for 1 wk with vector, K-Ras12V, a nonphosphorylatable mutant (K-Ras12V181A), or mitochondrially targeted K-Ras (Mas70–K-Ras12V) were able to produce stable clones that grew to confluence after replating (Fig. 1*B*). Cells expressing phosphomimetic K-Ras12V181E did not survive (Fig. 1*B*). Strikingly, cells expressing ER-targeted M1–K-Ras12V behaved like K-Ras12V181E–expressing cells and could not be recovered in the clonogenic assay (Fig. 1*B*). The expression of all of the K-Ras constructs was similar at 24 h after transfection (Fig. 1*B*, *Lower*), indicating that toxicity did not correlate with expression levels. Whereas a phosphomimetic substitution at position 181 was required to render natively targeted K-Ras12V toxic, ER-targeted M1–K-Ras12V did not require a phosphomimetic substitution for toxicity, suggesting that enforced localization on the ER is sufficient. Neither was an activating G12V mutation required as long as K-Ras carried a phosphomimetic residue at position 181 (Fig. 1*C*), suggesting that the ability to cycle between GDP- and GTP-bound states remained intact. To confirm that the nucleotide-binding domain (amino acids 1–165, G domain) of K-Ras was required for toxicity, we extended GFP with the 20-aa C-terminal hypervariable region of K-Ras4B with or without a phosphomimetic substitution at position 181. Neither K-Ras tail had an effect on cell survival (Fig. 1*D*). These results show that phopho–K-Ras4B limits cell survival from the ER and suggest that the GTPase interacts with Bcl-xL on this compartment.

K-Ras Binds the C Terminus of $InsP_3$ Receptors in an Activation, Phosphoserine 181, and Bcl-xL–Dependent Manner. A major pro-survival function of Bcl-xL at the ER is to bind to and sensitize IP3Rs that mediate calcium exchange between the ER and the mitochondrial matrix (13) where calcium is required for efficient respiration and inhibition of autophagy (14). IP3Rs span the ER membrane six times and have large N-terminal and smaller C-terminal domains disposed toward the cytoplasm (Fig. 2*A*), both of which interact with proteins that regulate the channel (15). The Bcl-xL binding sites on IP3R were localized to the C terminus of the receptor (C) (13). We previously showed by coimmunoprecipitation (co-IP) and FRET that K-Ras binds to Bcl-xL in a GTP-dependent fashion, although no direct interaction was demonstrated (6). Using only bacterially expressed, recombinant proteins, we were unable to detect an interaction between GST–Bcl-xL and 6×His–K-Ras12V181E, suggesting that the interaction may be indirect. To determine if K-Ras binds to IP3R in the same region as does Bcl-xL, we used an in vitro system with GST-tagged IP3R1 C-terminal fragments (Fig. 2*A*) and K-Ras proteins produced in *Escherichia coli*. Whereas GST–IP3R1-C was capable of affinity-purifying recombinant, activated K-Ras with a phosphomimetic substitution at serine 181 (K-Ras12V181E), it did not interact with either activated H-Ras61L or K-Ras12V with a native C terminus or with an alanine substitution at residue 181 (K-Ras12V181A) (Fig. 2*B*, *Left*). These data demonstrate that phosphomimetic K-Ras binds to the C terminus of IP3R1. Strikingly, when recombinant 6×His-tagged Bcl-xL produced in Sf9 insect cells was added to the binding reaction, the amount of K-Ras12V181E affinity purified by the same amount of GST–IP3R1-C was dramatically enhanced (Fig. 2*B*, *Right*). Longer exposures of the immunoblot revealed that, whereas oncogenic K-Ras with a native HVR (K-Ras12V181S) bound GST–IP3R1-C in the presence of Bcl-xL (albeit to a lesser extent than phosphomimetic K-Ras12V181E), nonphosphorylatable K-Ras12V181A did not (Fig. S3), indicating that phosphorylation promoted binding.

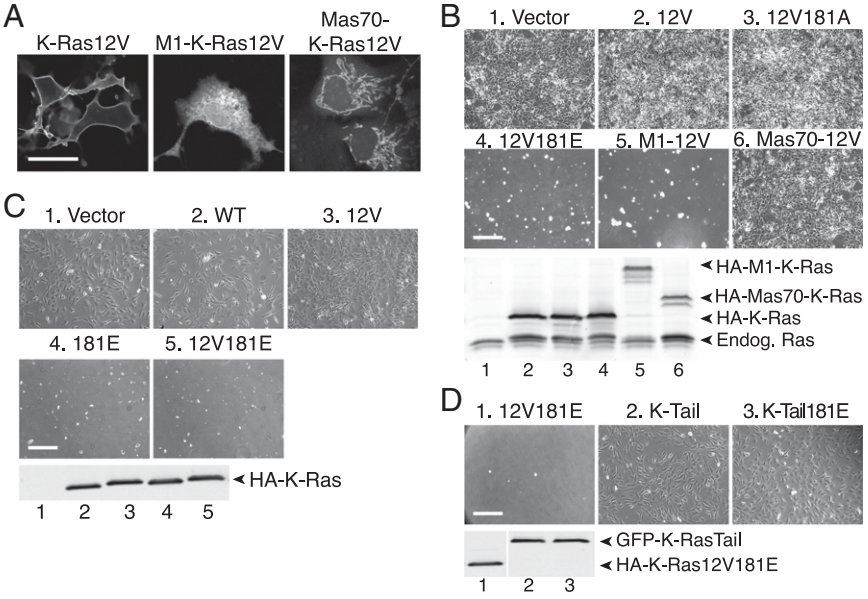

Fig. 1. Phospho–K-Ras inhibits cell survival from the ER. (*A*) Representative images of COS-1 cells expressing the indicated HA-tagged activated K-Ras construct and YFP-RBD. YFP-RBD fluorescence reports the localization of each K-Ras construct on plasma membrane (native targeting), ER (M1 tether), and mitochondria (Mas70 tether). (Scale bar, 15 μm.) (*B–D*, *Upper*) Representative phase contrast images of NIH 3T3 cells transfected with the indicated K-Ras constructs assessed for clonogenic survival as described in *Materials and Methods*. (Scale bar, 100 μm.) (*Lower*) Anti-PanRas immunoblot demonstrating equivalent expression of HA-tagged K-Ras constructs.

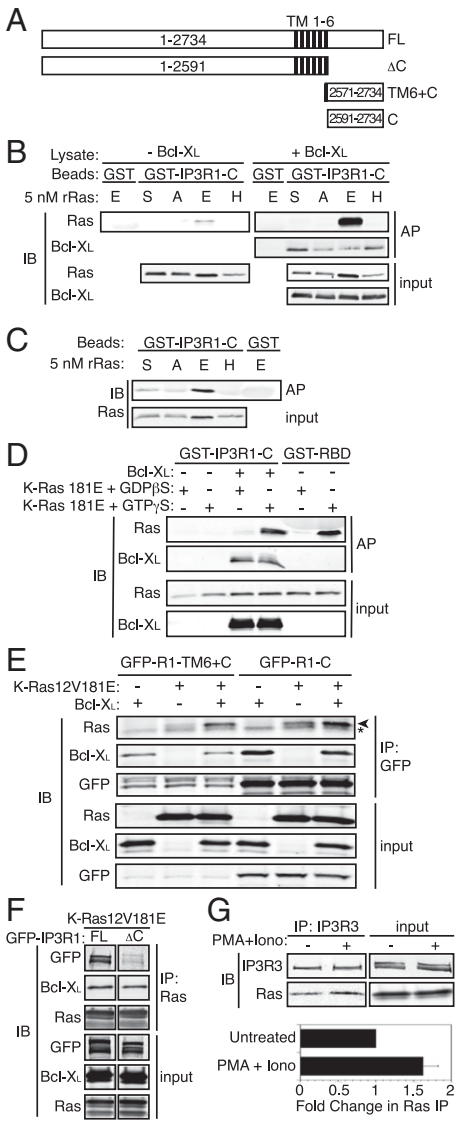

Fig. 2. K-Ras binds the C terminus of IP3R in an activation, amino acid 181 phosphomimetic- and Bcl-Xl–dependent fashion. (*A*) Schematic of full-length and truncation mutants of IP3R1. C, C terminus; FL, full length;.TM, transmembrane segments. (*B*) Affinity purification of recombinant Ras (5 nM) (A, K-Ras12V181A; E, K-Ras12V181E; H, H-Ras61L; S, K-Ras12V181S) with GST or GST–IP3R1-C in Sf9 cell lysates with or without baculovirus-expressed human Bcl-xL. Samples were immunoblotted with anti-PanRas and anti–Bcl-xL antibodies. (*C*) Affinity purification of 5 nM recombinant Ras with GST or GST–IP3R1-C in PBS + 1% Tx-100. Samples were immunoblotted with anti-PanRas antibody. (*D*) Affinity purification and analysis as in *B* using 5 nM recombinant K-Ras 181E loaded in vitro with GDPβS or GTPγS. (*E*) Immunopurification of GFP–IP3R1–TM6+C or GFP–IP3R1–C from COS-1 cell lysates with or without Bcl-xL and K-Ras 12V181E expression. Samples were immunoblotted with anti-PanRas, anti–Bcl-xL, and anti-GFP antibodies. Asterisk indicates Ig light chain. (*F*) Immunopurification of K-Ras 12V181E from COS-1 cell lysates from cells expressing Bcl-xL and either GFP–IP3R1 full-length or ΔC. Samples were analyzed as in *D*. (*G*, *Upper*) Immunopurification of endogenous IP3R3 from Panc-1 cell lysates. Cells were untreated or stimulated with 50 ng/mL PMA + 250 ng/mL ionomycin for 10 min. Samples were immunoblotted with anti-PanRas or anti-IP3R3 antibodies. (*Lower*) Quantification (Li-Cor) of Ras bands normalized to the IP3R3 bands in the co-IP. The *Lower* bar represents the fold change in immunodetectable Ras (mean ± SEM, $n = 4$).

In contrast to the effect of Bcl-xL on K-Ras12V181E binding, the presence of phosphomimetic K-Ras did not augment the amount of Bcl-xL affinity purified by GST–IP3R1-C (Fig. 2*B*, *Right*), suggesting that Bcl-xL binding to the C terminus of IP3R is permissive for K-Ras12V181E binding and promotes formation of a trimolecular complex in which both K-Ras12V181E and Bcl-xL bind directly to IP3R.

GST–IP3R1-C could affinity purify bacterially expressed K-Ras12V181E >> K-Ras12V > K-Ras12V181A, but failed to interact with H-Ras61L (Fig. 2*C*). Thus, phosphomimetic K-Ras12V181E interacts directly with the C terminus of IP3R1.

To determine if the GTP-bound state was required for phosphomimetic K-Ras to interact with IP3R, we produced 6×His-tagged K-Ras181E, which is wild type at codon 12, allowing for in vitro loading of specific guanine nucleotides. Subsequent to purification, K-Ras181E was loaded with either the nonhydrolyzable GDP analog GDPβS or the nonhydrolyzable GTP analog GTPγS. Affinity purification of GTPγS-loaded, but not GDPβS-loaded K-Ras181E with GST–Raf-1–RBD (Fig. 2*D*) demonstrated that the recombinant proteins were properly folded, efficiently bound guanine nucleotides, and behaved as expected with regard to activation state. GST–IP3R1-C was able to affinity purify GTPγS-loaded but not GDPβS-loaded K-Ras181E in the presence of recombinant Bcl-xL (Fig. 2*D*). These data demonstrate that only the active form of phosphomimetic K-Ras binds to IP3R. Coimmunoprecipitation analysis of GFP–R1–TM6+C or GFP–R1–C plus HA–K-Ras12V181E ± HA–Bcl-xL expressed in COS-1 cells confirmed the Bcl-xL–enhanced interaction of IP3R with phosphomimetic K-Ras (Fig. 2*E*). Concordant with the in vitro results (Fig. 2*B*), expression of K-Ras12V181E did not affect Bcl-xL binding. These results suggest that the K-Ras/Bcl-xL/IP3R complex forms in intact cells in which the C-terminal CAAX sequence of K-Ras is efficiently processed. Whereas the ability of the complex to form with recombinant K-Ras indicates that post-translational processing is not required for binding, CAAX processing in intact cells would likely be required for proper K-Ras localization to the ER membrane where it would encounter both Bcl-xL and IP3R.

Having demonstrated that the IP3R C terminus is sufficient for formation of the K-Ras/Bcl-xL/IP3R complex, we next sought to determine if it is necessary. We generated a full-length (FL) and a truncated (ΔC) form of GFP-tagged IP3R1 for use in coimmunoprecipitation experiments (Fig. 2*A*). GFP-IP3R1-FL but not GFP-IP3R1-ΔC was coimmunoprecipitated by K-Ras12V181E (Fig. 2*F*). These data show that the C terminus of IP3R is necessary for the formation of the K-Ras/Bcl-xL/IP3R complex. We next sought to demonstrate the ability of endogenous phospho–K-Ras to bind to endogenous IP3R. The human pancreatic adenocarcinoma cell line, Panc-1, which harbors an activated allele of K-Ras, was stimulated with phorbol myristate acetate (PMA) plus ionomycin to induce phosphorylation of S181. Immunoprecipitation of endogenous IP3R3 demonstrated a 60% increase in K-Ras binding after PKC activation (Fig. 2*G*). Thus, endogenous K-Ras interacts with endogenous IP3R, and this interaction is augmented by treatment with a PKC agonist.

Activated Phosphomimetic K-Ras Blocks the Ability of Bcl-xL to Sensitize IP3Rs. We previously showed by single-channel patch clamp electrophysiology that Bcl-xL sensitized IP3Rs to the activity of $InsP_3$ (13, 16). We therefore tested the effects of K-Ras on the activity of IP3R using the same method. Nuclei were isolated from a chicken pre–B-cell line (DT40) that is null for all three isoforms of chicken IP3Rs but is reconstituted with rat IP3R3. We measured channel open probability (P_O) in response to recombinant 6×His-tagged Ras proteins (K-Ras12V, K-Ras12V181A, K-Ras12V181E, and H-Ras61L) included in the patch pipette solution that bathes both N- and C-terminal domains of the channel, with or without the addition of recombinant Bcl-xL (Fig. 3 *A* and *B*). Consistent with previous work, channel gating in the presence of subsaturating (1 μM) $InsP_3$ was strongly enhanced by 1 μM recombinant Bcl-xL. Interestingly, in the absence of Bcl-xL, K-Ras12V181E but neither K-Ras12V nor K-Ras12V181A sensitized the channel to low [$InsP_3$], although to a much lesser extent than did Bcl-xL. Strikingly, K-Ras12V and K-Ras12V181E

blocked the ability of Bcl-xL to sensitize the receptor to $InsP_3$ (Fig. 3 *A* and *B*). In contrast, K-Ras12V181A and H-Ras61L had no effect, indicating that the functional effect is K-Ras specific and dependent on the residue at position 181. Similar results were obtained using endogenous IP3R in the nuclear envelope of Sf9 cells (Fig. S4). These data show that activated phosphomimetic K-Ras blocks an action of Bcl-xL on the IP3R that promotes cell survival (13, 16).

To allow for CAAX processing of K-Ras and ER targeting, we repeated these experiments in a system in which K-Ras was expressed from a plasmid rather than included in the patch pipette solution. Expression of K-Ras12V181E or M1–K-Ras12V, but not K-Ras12V181A, by baculoviral infection of Sf9 cells, strongly inhibited the ability of Bcl-xL to sensitize the channel to $InsP_3$ (Fig. 3*C*). Thus, both CAAX- and M1-targeted K-Ras were able to block the action of Bcl-xL. Importantly, whereas K-Ras12V required a phosphomimetic residue at position 181 to block the ability of Bcl-xL to activate the channel, M1–K-Ras12V did not, suggesting that forced localization to the ER membrane eliminates the requirement for phosphorylation. This result is concordant with the cell toxicity results described above (Fig. 1*B*).

Because the phospho–K-Ras C-terminal "tail" was required for the effects of K-Ras on IP3R, we next tested if the tail alone was sufficient. We synthesized 19 amino acid peptides corresponding to the tails of K-Ras181S (wild type), K-Ras181A (nonphosphorylatable), and K-Ras181E (phosphomimetic). Like K-Ras, Rap1a is targeted to membranes by virtue of prenylation and a polybasic sequence. Accordingly, a corresponding peptide based on the Rap1a C terminus was used as an additional control. Addition of K-Ras181E tail peptide alone did not affect IP3R channel activity activated by 1 μM $InsP_3$ (Fig. 3*D*). Furthermore, none of the peptides added alone affected the ability of Bcl-xL to sensitize IP3Rs. In contrast, the K-Ras181E tail peptide completely inhibited the ability of full-length K-Ras12V181E to block the sensitizing effect of Bcl-xL (Fig. 3*D*). The K-Ras181S tail peptide showed modest activity in this regard, but K-Ras181A and Rap1a tail peptides were without effect. These data suggest that the C-terminal peptide that corresponds to phosphomimetic K-Ras can compete for binding of the full-length protein to the IP3R. Because GTP-loaded K-Ras181E is required for the interaction (Fig. 2*D*), these results suggest that both the G domain and the C terminus participate in the binding of K-Ras12V181E to the IP3R in the presence of Bcl-xL. Taken together, these data demonstrate that activated, phosphomimetic K-Ras can block the ability of Bcl-xL to sensitize the IP3R and thereby promote cell survival.

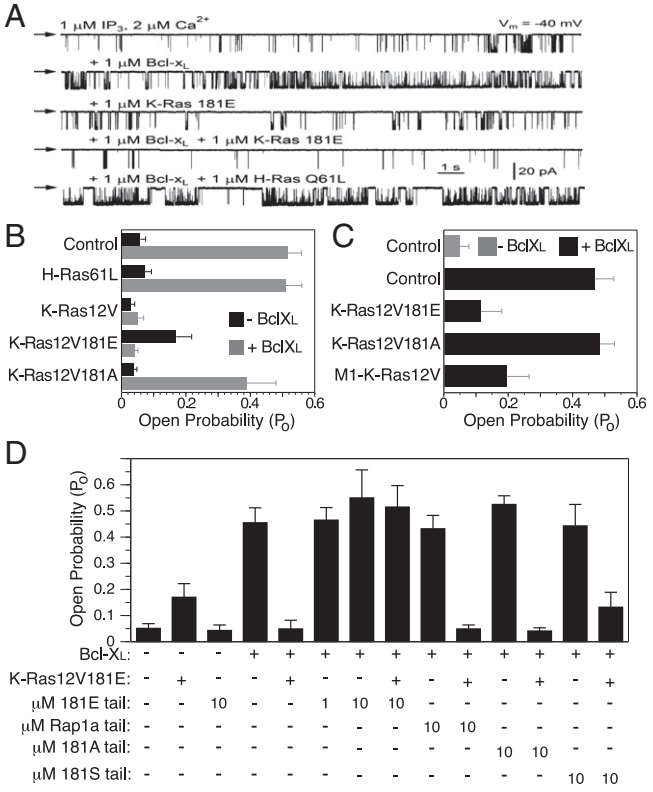

Fig. 3. Activated K-Ras with a phosphomimetic amino acid at position 181 blocks the ability of Bcl-xL to sensitize IP3Rs. (*A*) Representative current traces of rat IP3R3 channel activity measured by patch clamp electrophysiology of nuclei isolated from stable rat IP3R3 expressing DT40 cells null for all three chicken IP3Rs. Downward deflections indicate channel openings. Arrows indicate zero-current level. Specified molecules present in the pipette solution. All pipette solutions contained 1 μM $InsP_3$ and 2 μM free Ca^{2+}. (*B*) Summary of IP3R3 open probability (P_o) in response to 1 μM $InsP_3$ and 2 μM free Ca^{2+} in the presence of 1 μM recombinant Ras with or without 1 μM recombinant Bcl-xL. (*C*) Summary of endogenous Sf9 cell IP3R P_o in isolated nuclei from Sf9 cells 48 h postinfection with indicated recombinant baculovirus. Pipette solutions contained 10 nM IP_3 and 2 μM Ca^{2+} with or without 1 μM recombinant Bcl-xL. (*D*) Summary of P_o of rat IP3R3 in response to 1 μM $InsP_3$ and 2 μM free Ca^{2+} (as in *B*) in presence of indicated concentrations of K-Ras or Rap1a tail peptides with or without 1 μM recombinant K-Ras 12V181E and/or 1 μM recombinant Bcl-xL. (*B–D*) Bars represent mean ± SEM, $n \geq 4$ for *B* and *C* and $n \geq 5$ for *D*.

Activated Phosphomimetic K-Ras Diminishes Mitochondrial $[Ca^{2+}]$. To determine directly the effects of activated, phosphomimetic K-Ras on $[Ca^{2+}]$ in the mitochondrial matrix we used mt-pericam, a genetically encoded fluorescent calcium sensor that incorporates a mitochondrial targeting sequence (Fig. 4*A*) (17). We coexpressed mt-pericam in MEFs with vector, K-Ras12V, or K-Ras12V181E. In wild-type MEFs, expression of K-Ras12V181E, and to a lesser extent K-Ras12V, diminished mitochondrial $[Ca^{2+}]$ (Fig. 4 *B* and *C*). The basal mitochondrial $[Ca^{2+}]$ in Bcl-$xL^{-/-}$ MEFs was similar to that of Bcl-$xL^{+/+}$ MEFs, suggesting that, in the course of adaptation to growth without Bcl-xL, these cells use an alternate means of assuring adequate delivery of calcium to the mitochondria. Importantly, neither K-Ras12V nor K-Ras12V181E had any effect on mitochondrial $[Ca^{2+}]$ in Bcl-$xL^{-/-}$ MEFs (Fig. 4 *B* and *C*). When Bcl-xL was expressed exogenously in the Bcl-$xL^{-/-}$ MEFs, they regained sensitivity to K-Ras12V and K-Ras12V181E with regard to decreases in mitochondrial $[Ca^{2+}]$ (Fig. 4 *B* and *C*). Thus, active, phosphomimetic K-Ras12V181E diminishes $[Ca^{2+}]$ in the mitochondrial matrix in a Bcl-xL–dependent fashion, consistent with its effects on the ability of Bcl-xL to sensitize IP3Rs.

Phospho–K-Ras Induces Autophagy in a Bcl-xL–Dependent Manner. Because constitutive release of calcium from IP3Rs is required to suppress autophagy (14) and because K-Ras12V181E expression altered mitochondrial calcium homeostasis, we sought to determine if activated, phosphomimetic K-Ras induces autophagy. Scoring for autophagy with vesicular accumulation of mCherry-LC3 we found that Bcl-$xL^{+/+}$ MEFs transfected with either K-Ras12V181E or M1–K-Ras12V demonstrated a twofold increase in the percent of autophagic cells over vector control (Fig. S5*A*). Expression of neither K-Ras12V181E nor M1–K-Ras12V increased the appearance of autophagosomes in Bcl-$xL^{-/-}$ cells but ectopic expression of Bcl-xL in Bcl-$xL^{-/-}$ MEFs restored sensitivity (Fig. S5*A*). We confirmed this effect with endogenous, activated phospho–K-Ras using the isogenic HCT116 cells described above (Fig. S2*B*). HCT116 K-Ras WT and 13D cells were transfected with mCherry-LC3 and then treated with ionomycin, PMA plus ionomycin, or Aplog-1 (a potent analog of the PKC agonist Bryostatin-1) (18) for 24 h (Fig. S5 *B* and *C*). HCT116 K-Ras13D cells treated with aplog-1 revealed threefold more autophagic cells relative to HCT116 K-Ras WT cells (Fig. S5 *B* and *C*). Transmission electron micrographs confirmed that Aplog-1–treated cells contained double-membrane–bound autophagosomes (Fig. S5*D*).

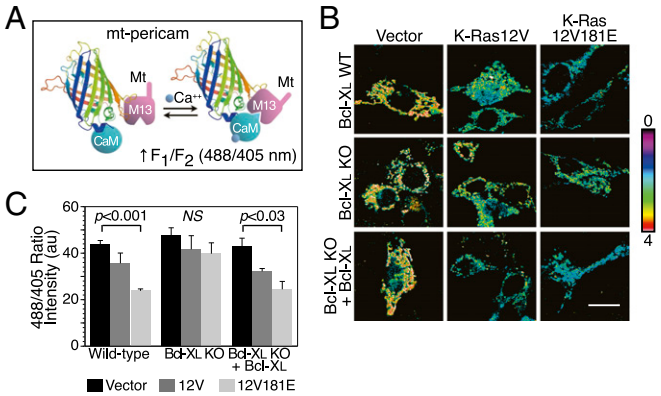

Fig. 4. Activated K-Ras with a phosphomimetic amino acid at position 181 diminishes mitochondrial [Ca^{2+}]. (*A*) Schematic representation of mt-pericam calcium reporter. Shown is the circularly permuted GFP barrel structure with a calmodulin (CaM) domain appended to the N terminus and an M13 CaM binding domain together with a mitochondrial targeting sequence (mt) appended to the C terminus. Calcium induces intramolecular binding, which contorts the fluorophore and increases the 488/405 excitation ratio fluorescence at 510 nm. (*B*) Representative 488/405 ratio images of Bcl-$xL^{+/+}$, $^{-/-}$, and rescued MEFs expressing mt-pericam and the indicated construct. Higher ratio (indicated by color look-up-table) indicates higher mitochondrial [Ca^{2+}]. (Scale bar, 10 μm.) (*C*) Quantification of single cell ratio intensities in *B*. Data plotted are mean ± SEM, $n = 3$, *P* values as indicated; ≥10 cells measured per condition per experiment.

$Atg5^{+/-}$ MEFs heterozygous for the critical autophagy gene Atg5 (19) were partially protected from K-Ras12V181E-mediated toxicity (Fig. S5*E*). These results suggest that expression of phosphomimetic, oncogenic Ras induces autophagy, which in turn is required for poor survival.

Discussion

The observation that PKC agonists induce rapid translocation of K-Ras4B from the plasma membrane to intracellular compartments led to the discovery that this Ras isoform can be phosphorylated in its membrane targeting domain (6). A large body of evidence supports a model whereby the polybasic region of K-Ras4B contributes to membrane affinity through an electrostatic interaction with the inner leaflet of the plasma membrane (4, 5, 20, 21). Phosphorylation of serine 181 sufficiently weakens this interaction to cause K-Ras4B to dissociate from the plasma membrane. Since the initial report of this farnesyl-electrostatic switch (6), other small GTPases that associate with membranes via polybasic regions that operate in conjunction with prenylation, including RalA (22) and Rnd3 (23), have been shown to be substrates for kinases that modulate membrane association through a similar prenyl-electrostatic switch.

The accumulation of phospho–K-Ras on endomembrane may reflect the fact that CAAX proteins that lack a second signal (palmitoylation or a polybasic region) accumulate on ER and Golgi (4, 24, 25). More surprising than the endomembrane localization of phospho–K-Ras4B was the observation that its translocation was associated with cell death (6). The localization of phospho–K-Ras4B on the OMM suggested that cell toxicity might be related to apoptosis; however, the requirement for Bcl-xL for phospho–K-Ras4B–mediated toxicity clouded the picture considerably. The results reported here explain the earlier findings. Using multiple well-established assays, we determined that expression of phosphomimetic K-Ras12V181E did not activate the intrinsic mitochondrial apoptosis pathway. Nevertheless, a clonogenic assay revealed that phosphomimetic K-Ras4B limits cell survival. Using K-Ras4B constructs stringently targeted to various subcellular compartments, we found that the toxicity of K-Ras12V181E depended on its localization at the ER and could not be elicited by targeting it to the OMM.

In addition to inhibiting proapoptotic proteins that act at mitochondria to induce permeability transition, Bcl-2 and Bcl-xL have well-established antiapoptotic activities at the ER, albeit through distinct mechanisms (12). High levels of calcium leaking from the ER into the cytoplasm can initiate cell death through a variety of mechanisms that include triggering of OMM permeabilization to induce apoptosis (26, 27) and activation of calpain and other proteases to induce necrosis (28, 29). Bcl-2 can inhibit this relatively high leak into the cytoplasm by binding to the N terminus of IP3Rs and negatively regulating the channels (30, 31). Conversely, calcium flux from the ER to the mitochondria through IP3Rs is essential for mitochondrial respiratory function and cell survival. Bcl-xL binds to the C terminus of IP3Rs and sensitizes them for calcium transfer to mitochondria (13, 14, 16). The involvement of the ER and Bcl-xL in the toxicity of phosphomimetic K-Ras12V181E suggested that interference with mitochondrial calcium homeostasis might underlie the mechanism of toxicity.

We show that K-Ras4B interacts directly with the C terminus of IP3R. This is the same region to which Bcl-xL binds, sensitizing the receptor to $InsP_3$ and thereby enhancing cell survival (13, 14, 16). The interaction of K-Ras4B with IP3R requires it to be GTP bound, and it is enhanced when a phosphomimetic group is incorporated at residue 181. The requirement for GTP-binding suggests that the GTPase effector domain is involved in the interaction. However, the enhancement with a phosphomimetic and the ability of a peptide based on the C terminus of K-Ras4B to block the functional interaction with IP3R suggest that the interaction also depends on the C terminus of K-Ras4B. Perhaps most intriguing is the observation that this interaction is markedly enhanced in the presence of Bcl-xL. We previously reported that Bcl-xL could be coimmunoprecipitated with phospho–K-Ras4B (6); however, the affinity was low and no direct interaction was documented. Using a fully recombinant system, we found no evidence for a direct interaction between K-Ras4B and Bcl-xL. Thus, it appears that Bcl-xL interacts indirectly with K-Ras4B in a trimolecular complex with the C terminus of IP3R. Moreover, our data support a model whereby the binding of K-Ras4B to IP3R is greatly facilitated by prior binding of Bcl-xL, but the converse is not true. Thus, Bcl-xL binding to IP3R acts to allosterically regulate K-Ras4B binding.

The functional effects of these interactions on IP3R channel activity observed by nuclear patch clamp electrophysiology are entirely consistent with the binding data. The addition of recombinant phosphomimetic K-Ras12V181E protein to the patch pipette solution or overexpressing K-Ras12V181E in the cell before patch clamping the nuclear envelope blocked completely the ability of Bcl-xL to sensitize IP3Rs to $InsP_3$. In contrast, Ras12V181A had no such effect, demonstrating that the phosphomimetic residue is required. Thus, K-Ras12V181E binding to IP3R, an interaction facilitated by prior binding of Bcl-xL, blocks the prosurvival action of Bcl-xL on IP3R activity. This model was further supported by the observation that expression of Ras12V181E, but not Ras12V181A, led to decreased levels of mitochondrial [Ca^{2+}] in a Bcl-xL–dependent fashion.

Autophagy is a cellular process that evolved to promote cell survival by providing a way to derive energy and essential nutrients from the breakdown of excess cytoplasmic components (32). Calcium signaling is an important mechanism that regulates autophagy (33). We recently showed that the constitutive flux of calcium from the ER to mitochondria through IP3Rs is essential to suppress autophagy under conditions of abundant nutrients (14). The inhibition of this transfer by Ras12V181E can therefore account for the observed stimulation of autophagy in cells expressing Ras12V181E. In this context, the requirement for Atg5 for Ras12V181E-mediated toxicity may seem paradoxical. However, autophagy has also be associated with programmed cell death (34, 35) and our data suggest that autophagy caused by expression of phospho–K-Ras4B in the presence of Bcl-xL may play a role in limiting cell survival.

Effectors of small GTPases like K-Ras4B are defined as proteins that preferentially bind to the GTP-bound form of the

GTPase and, in so doing, undergo a functional change. Our data therefore establish IP3Rs as previously unappreciated effectors of K-Ras4B. The restriction of IP3Rs to the ER offers yet another example of spatially regulated Ras signaling (36). Most pathways regulated by Ras proteins promote cell survival and growth, although alternative signaling for cell death is a well-described paradigm (37). The fact that phosho–K-Ras4B signaling through IP3Rs at the ER promotes cell death suggests that this pathway could be exploited to develop anticancer therapeutics.

Materials and Methods

Clonogenic Survival Assay. Cells were transfected using Lipofectamine 2000 (Invitrogen) according to the manufacturer's protocol and cultured in selection media for at least 7 d. Cell survival was assessed by visual inspection. Colonies were dispersed by trypsinization and replating to produce a confluent monolayer suitable for imaging. Cells were imaged by phase contrast with a 10× objective using MetaMorph software (Molecular Devices).

Affinity Purification. GST-tagged proteins immobilized on beads were equivalently added to 1 mL of 1 mg/mL Sf9 lysate with or without Bcl-xL expression. Recombinant Ras was added to a final concentration of 5 nM. Beads were washed with PBS + 1% Tx-100 and eluted in 2× Laemmli buffer. Samples were analyzed by SDS/PAGE and immunoblot.

Electrophysiology. DT40 and Sf9 cells were suspended in a nuclear isolation solution containing 150 mM KCl, 250 mM sucrose, 1.5 mM β-mercaptoethanol, 10 mM Tris·HCl pH 7.5, 0.05 mM PMSF, and a protease inhibitor mixture (Roche). Nuclei were isolated using a Dounce glass homogenizer and plated onto a 1-mL glass bottomed dish containing standard bath solution [140 mM KCl, 10 mM Hepes, and 0.5 mM BAPTA (free $[Ca^{2+}]$ = 300 nM), pH 7.1]. The pipette solution contained 140 mM KCl, 0.5 mM ATP, 10 mM Hepes, pH 7.1. Ras baculoviruses were generated using the Bac-to-Bac baculovirus expression system (Invitrogen). Tail peptides were synthesized and HPLC purified by Genemed Synthesis and stored in TBS. Data were acquired using an Axopatch-1D amplifier (Axon Instruments), and single-channel analysis was performed using QuB software (University of Buffalo).

Mt-Pericam Microscopy. MEFs were cotransfected in a 4:1 ratio of the indicated pCGN plasmid to pcDNA3.1-mt-pericam [a gift from D. Clapham (Harvard Medical School, Boston) with permission from A. Miyawaki (Riken Brain Science Institute, Tokyo)]. Fluorescent images were acquired on a Zeiss LSM 510 Meta confocal microscope using a 63× objective. Mt-pericam fluorescence was excited with 405-nm and 488-nm lasers and detected at 515 nm according to published methods (38). Ratio images of fluorescent intensity (488/405) were generated and average ratio intensities of single cells were quantified using MetaMorph.

LC3 Translocation Assay. Cells were cotransfected in a 4:1 ratio of the indicated pCGN plasmid to pCherry-LC3. Four hours posttransfection, cells were treated with or without the indicated compounds (10 mM 3-methyladenine, 250 ng/mL ionomycin ± 50 ng/mL PMA, or 10 μM Aplog-1). Twenty-four hours after drug treatment, cells were fixed in 4% (wt/vol) paraformaldehyde (Electron Microscopy Sciences) and mounted on glass slides. Cells were scored positive for nuclear clearing of pCherry-LC3 or presence of >10 autophagic puncta.

ACKNOWLEDGMENTS. We thank Kazuhiro Irie for the kind gift of Aplog-1, David Sabatini for assistance with EMs, and Michelle Krogsgaard for her assistance in preparing recombinant proteins. This work was supported by National Institutes of Health Grants CA116034 and GM055279 and funding from the Jeffrey Rosenzweig Foundation for Pancreatic Cancer Research and the Children's Tumor Foundation (to M.R.P.) and GM056328 and MH059937 (to J.K.F.).

1. Bos JL (1989) ras oncogenes in human cancer: A review. *Cancer Res* 49(17):4682–4689.
2. Prior IA, Lewis PD, Mattos C (2012) A comprehensive survey of Ras mutations in cancer. *Cancer Res* 72(10):2457–2467.
3. Wright LP, Philips MR (2006) Thematic review series: Lipid posttranslational modifications. CAAX modification and membrane targeting of Ras. *J Lipid Res* 47(5): 883–891.
4. Choy E, et al. (1999) Endomembrane trafficking of ras: The CAAX motif targets proteins to the ER and Golgi. *Cell* 98(1):69–80.
5. Hancock JF, Paterson H, Marshall CJ (1990) A polybasic domain or palmitoylation is required in addition to the CAAX motif to localize p21ras to the plasma membrane. *Cell* 63(1):133–139.
6. Bivona TG, et al. (2006) PKC regulates a farnesyl-electrostatic switch on K-Ras that promotes its association with Bcl-XL on mitochondria and induces apoptosis. *Mol Cell* 21(4):481–493.
7. McLaughlin S, Aderem A (1995) The myristoyl-electrostatic switch: A modulator of reversible protein-membrane interactions. *Trends Biochem Sci* 20(7):272–276.
8. Wei MC, et al. (2001) Proapoptotic BAX and BAK: A requisite gateway to mitochondrial dysfunction and death. *Science* 292(5517):727–730.
9. Shirasawa S, Furuse M, Yokoyama N, Sasazuki T (1993) Altered growth of human colon cancer cell lines disrupted at activated Ki-ras. *Science* 260(5104):85–88.
10. Chiu VK, et al. (2002) Ras signalling on the endoplasmic reticulum and the Golgi. *Nat Cell Biol* 4(5):343–350.
11. Pfanner N, Geissler A (2001) Versatility of the mitochondrial protein import machinery. *Nat Rev Mol Cell Biol* 2(5):339–349.
12. Chipuk JE, Moldoveanu T, Llambi F, Parsons MJ, Green DR (2010) The BCL-2 family reunion. *Mol Cell* 37(3):299–310.
13. White C, et al. (2005) The endoplasmic reticulum gateway to apoptosis by Bcl-X(L) modulation of the InsP3R. *Nat Cell Biol* 7(10):1021–1028.
14. Cárdenas C, et al. (2010) Essential regulation of cell bioenergetics by constitutive InsP3 receptor Ca2+ transfer to mitochondria. *Cell* 142(2):270–283.
15. Foskett JK, White C, Cheung KH, Mak DO (2007) Inositol trisphosphate receptor Ca2+ release channels. *Physiol Rev* 87(2):593–658.
16. Li C, et al. (2007) Apoptosis regulation by Bcl-x(L) modulation of mammalian inositol 1,4,5-trisphosphate receptor channel isoform gating. *Proc Natl Acad Sci USA* 104(30): 12565–12570.
17. Nagai T, Sawano A, Park ES, Miyawaki A (2001) Circularly permuted green fluorescent proteins engineered to sense Ca2+. *Proc Natl Acad Sci USA* 98(6):3197–3202.
18. Nakagawa Y, et al. (2009) A simple analogue of tumor-promoting aplysiatoxin is an antineoplastic agent rather than a tumor promoter: Development of a synthetically accessible protein kinase C activator with bryostatin-like activity. *J Am Chem Soc* 131(22):7573–7579.
19. Kuma A, et al. (2004) The role of autophagy during the early neonatal starvation period. *Nature* 432(7020):1032–1036.
20. Roy MO, Leventis R, Silvius JR (2000) Mutational and biochemical analysis of plasma membrane targeting mediated by the farnesylated, polybasic carboxy terminus of K-ras4B. *Biochemistry* 39(28):8298–8307.
21. Yeung T, et al. (2008) Membrane phosphatidylserine regulates surface charge and protein localization. *Science* 319(5860):210–213.
22. Kashatus DF, et al. (2011) RALA and RALBP1 regulate mitochondrial fission at mitosis. *Nat Cell Biol* 13(9):1108–1115.
23. Madigan JP, et al. (2009) Regulation of Rnd3 localization and function by protein kinase C alpha-mediated phosphorylation. *Biochem J* 424(1):153–161.
24. Michaelson D, Ahearn I, Bergo M, Young S, Philips M (2002) Membrane trafficking of heterotrimeric G proteins via the endoplasmic reticulum and Golgi. *Mol Biol Cell* 13(9):3294–3302.
25. Yeung T, et al. (2006) Receptor activation alters inner surface potential during phagocytosis. *Science* 313(5785):347–351.
26. Hanson CJ, Bootman MD, Roderick HL (2004) Cell signalling: IP3 receptors channel calcium into cell death. *Curr Biol* 14(21):R933–R935.
27. Rizzuto R, et al. (2003) Calcium and apoptosis: Facts and hypotheses. *Oncogene* 22(53):8619–8627.
28. Kitsis RN, Molkentin JD (2010) Apoptotic cell death "Nixed" by an ER-mitochondrial necrotic pathway. *Proc Natl Acad Sci USA* 107(20):9031–9032.
29. Zong WX, Thompson CB (2006) Necrotic death as a cell fate. *Genes Dev* 20(1):1–15.
30. Chen R, et al. (2004) Bcl-2 functionally interacts with inositol 1,4,5-trisphosphate receptors to regulate calcium release from the ER in response to inositol 1,4,5-trisphosphate. *J Cell Biol* 166(2):193–203.
31. Rong YP, et al. (2009) The BH4 domain of Bcl-2 inhibits ER calcium release and apoptosis by binding the regulatory and coupling domain of the IP3 receptor. *Proc Natl Acad Sci USA* 106(34):14397–14402.
32. Ohsumi Y (2001) Molecular dissection of autophagy: Two ubiquitin-like systems. *Nat Rev Mol Cell Biol* 2(3):211–216.
33. Harr MW, Distelhorst CW (2010) Apoptosis and autophagy: Decoding calcium signals that mediate life or death. *Cold Spring Harb Perspect Biol* 2(10):a005579.
34. Baehrecke EH (2005) Autophagy: Dual roles in life and death? *Nat Rev Mol Cell Biol* 6(6):505–510.
35. Høyer-Hansen M, Bastholm L, Mathiasen IS, Elling F, Jäättelä M (2005) Vitamin D analog EB1089 triggers dramatic lysosomal changes and Beclin 1-mediated autophagic cell death. *Cell Death Differ* 12(10):1297–1309.
36. Fehrenbacher N, Bar-Sagi D, Philips M (2009) Ras/MAPK signaling from endomembranes. *Mol Oncol* 3(4):297–307.
37. Cox AD, Der CJ (2003) The dark side of Ras: Regulation of apoptosis. *Oncogene* 22(56): 8999–9006.
38. Shimozono S, et al. (2002) Confocal imaging of subcellular Ca2+ concentrations using a dual-excitation ratiometric indicator based on green fluorescent protein. *Sci STKE* 2002(125):pl4.